J|A|C|S ARTICLES

Published on Web 01/19/2010

Solvent-Induced Transformation of Single Crystals of a Spin-Crossover (SCO) Compound to Single Crystals with Two Distinct SCO Centers

Bao Li,[†] Rong-Jia Wei,[†] Jun Tao,*[,†] Rong-Bin Huang,[†] Lan-Sun Zheng,[†] and Zhiping Zheng*[,‡]

State Key Laboratory of Physical Chemistry of Solid Surfaces, College of Chemistry and Chemical Engineering, Xiamen University, Xiamen 361005, People's Republic of China, and Department of Chemistry, University of Arizona, Tucson, Arizona 85721

Received August 2, 2009; E-mail: taojun@xmu.edu.cn; zhiping@u.arizona.edu

Abstract: The long-sought-after crystal structure of Fe(tpa)$(NCS)_2$ (**1**, tpa = tris(2-pyridylmethyl)amine), an otherwise well-studied spin-crossover (SCO) complex, has been obtained, and its one-step, incomplete spin transition was correlated to its solid-state structures at different temperatures. Upon exposure to methanol vapor, single-crystal-to-single-crystal transformation of **1** to a new SCO compound, **2**, formulated as {[Fe(tpa)$(NCS)_2$]·[Fe(tpa)$(NCS)_2$·CH_3OH]}, occurs with a dramatic color change from yellow to red. Crystallographic studies revealed that the asymmetric unit of the structure of **2** contains two independent Fe(II) centers. Studies by magnetic measurements and Mössbauer spectroscopy revealed a two-step complete spin transition for compound **2**, between LS−LS and HS−HS, via an unambiguous intermediate LS−HS phase; the two SCO centers of disparate spin states were resolved crystallographically. That a significant portion of the original crystal structure is maintained indicates that the present approach is a more subtle means of altering the properties associated with SCO phenomenon than by changing counteranions or crystallization using different solvents. Furthermore, the dramatic changes in crystal structure and SCO behaviors triggered by mere solvent sorption suggest that this approach is rather efficient in modifying and hopefully fine-tuning and optimizing properties of SCO compounds. Coupled with the aforementioned gentleness and subtlety, the present approach of heterogeneously introducing perturbations to pre-existing supramolecular arrays of SCO units is more conducive to systematic studies aiming at the discovery of new SCO systems and phenomenon toward their ultimate materials applications.

Introduction

Spin-crossover (SCO) compounds, characterized by their ability to switch between different electronic spin states upon certain condition changes, are a class of fundamentally interesting substances.[1] Frequently accompanying the spin transition, dramatic changes of properties (color, magnetism) occur,[2] based on which significant applications of these materials as molecular switches and sensors for information storage and in display technologies have been envisioned. A large number of SCO compounds have appeared in the literature, among which octahedral Fe(II) and Fe(III) complexes are arguably most extensively studied.[3] Over the course of these studies, it has become clear that SCO behaviors incorporating hysteresis phenomenon that are important for the aforementioned technological applications are dependent on how individual SCO centers interact, both intramolecularly and intermolecularly.[4,5a,b] Great efforts have thus been made to enhance cooperativity between SCO centers in order to achieve abrupt SCO transitions and significant bistability.[1,4] Molecularly, the rational design of ligands for the bridging of individual metal centers has enjoyed much attention. On the other hand, extensive efforts have been made to manipulate the noncovalent interaction between different SCO complex units in the solid state, for example, by changing crystallization solvents or counteranions.[6,7] Both single- and two-step spin-transition behaviors have been reported, and the nature of the various phases involved has been

[†] Xiamen University.
[‡] University of Arizona.

(1) (a) Shultz, D. A. In *Magnetism: Molecules to Materials II*; Miller, J. S., Drillon, M., Eds.; Wiley-VCH: Weinheim, Germany, 2001; p 281. (b) Gütlich, P.; Goodwin, H. A. *Top. Curr. Chem.* **2004**, *234*, 1–276.

(2) (a) Kahn, O.; Launay, J. P. *Chemtronics* **1988**, *3*, 140–151. (b) Sato, O.; Iyoda, T.; Fujishima, A.; Hashimoto, K. *Science* **1996**, *272*, 704–705. (c) Gütlich, P.; Garcia, Y.; Woike, T. *Coord. Chem. Rev.* **2001**, *219−221*, 839–879. (d) Sato, O.; Tao, J.; Zhang, Y.-Z. *Angew. Chem., Int. Ed.* **2007**, *46*, 2152–2187.

(3) (a) Gütlich, P.; Garcia, Y.; Goodwin, H. A. *Chem. Soc. Rev.* **2000**, *29*, 419–427. (b) Bai, Y.-L.; Tao, J.; Huang, R.-B.; Zheng, L.-S.; Zheng, S.-L.; Oshida, K.; Einaga, Y. *Chem. Commun.* **2008**, 1753–1755. (c) Tao, J.; Maruyama, H.; Sato, O. *J. Am. Chem. Soc.* **2006**, *128*, 1790–1791. (d) Li, B.; Tao, J.; Sun, H.-L.; Sato, O.; Huang, R.-B.; Zheng, L.-S. *Chem. Commun.* **2008**, 2269–2271. (e) Li, B.; Yang, F.-L.; Tao, J.; Sato, O.; Huang, R.-B.; Zheng, L.-S. *Chem. Commun.* **2008**, 6019–6021.

(4) (a) Létard, J. F.; Guionneau, P.; Goux-Capes, L. *Top. Curr. Chem.* **2004**, *235*, 221–249. (b) Murray, K. S.; Kepert, C. J. *Top. Curr. Chem.* **2004**, *233*, 195–228.

(5) (a) Kepenekian, M.; Le Guennic, B.; Robert, V. *J. Am. Chem. Soc.* **2009**, *131*, 11498–11502. (b) Kepenekian, M.; Le Guennic, B.; Robert, V. *Phys. Rev. B* **2009**, *79*, 094428/1−094428/5. (c) Sherrill, C. D.; Sumpter, B. G.; Sinnokrot, M. O.; Marshall, M. S.; Hohenstein, E. G.; Walker, R. C.; Gould, I. R. *J. Comput. Chem.* **2009**, *30*, 2187–2193.

 10.1021/ja909695f

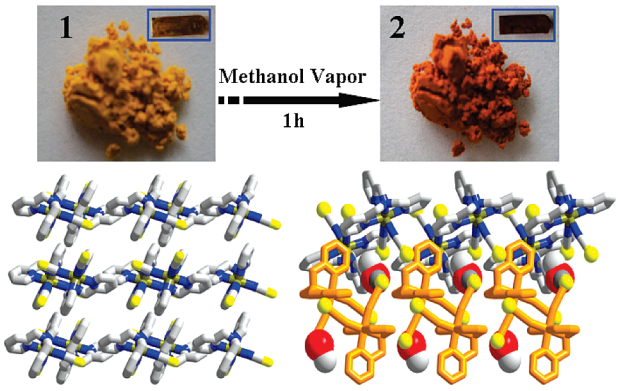

Figure 1. Color change upon methanol sorption (top) and crystal-packing modes (bottom) of **1** (left) and **2** (right).

investigated. In a small number of cases, the intermediate phase between the LS and HS extremes has also been identified, either as a mixture of HS and LS on the same metal site or consisting of two crystallographically independent SCO centers in different spin states.[8−11]

We have recently obtained the long-sought-after single crystals of Fe(tpa)$(NCS)_2$ (**1**, tpa = tris(2-pyridylmethyl)amine), a well-studied mononuclear SCO complex.[12] Structural determination reveals an ordered two-dimensional (2-D) arrangement of individual molecules of Fe(tpa)$(NCS)_2$, via hydrogen bonding and $\pi-\pi$ interactions in one direction and hydrogen bonding only in the other (Figure 1). The rather open structure prompted us to look at the possibility of introducing guest species that may disrupt the pre-existing noncovalent interactions and in so doing to modify the properties of an otherwise well-researched SCO compound. Approaches such as changing counteranions or recrystallization solvents have been commonly used to achieve different solid-state cooperativity between SCO centers,[6,7,13] but they tend to cause complete disintegration of the original supramolecular interactions. Coupled with the complexity and subtlety of various noncovalent interactions, such "brute-force" approaches are not conducive for systematic studies aiming at fine-tuning and optimization of SCO properties based on the same basic SCO complex unit. In other words, though interesting results are obtained from such studies, they are more likely to be isolated, and any attempts to draw general conclusions regarding structure−property relationship of these materials are sketchy at best.

As our initial efforts to provide a solution to the aforementioned problems, we report here a distinct approach, one by which the property of a SCO complex can be modified via partial interruption to its pre-existing supramolecular interactions. Specifically, we submit that *heterogeneously* introducing certain guest molecules that are capable of competitive noncovalent interactions with the SCO complex would result in partial and localized disruption to its pre-existing intermolecular interactions and, therefore, noticeable changes to its spin-transition activation barrier.[6] The perturbation introduced is so subtle that only part of the original structure is altered and that single crystals of the original compound may be directly transformed into a new structure wherein the SCO sites are engaged in interactions distinctly different from those present in the original structure. For example, volatile solvents capable of hydrogen bonding or $\pi-\pi$ interactions may be absorbed by single crystals whose packing involves such noncovalent forces.[6] Alternatively, this process may be accomplished by soaking the original crystals in a suitable solvent or solvent mixture, provided that the compound is insoluble; the solvent molecules are changed into the original crystal structure, affording new crystalline phases but with a significant portion of the original supramolecular interactions retained. This method, causing only gradual transformation to the original crystalline phase, is expected to be more conducive to systematic studies aiming at the optimization of SCO properties based on a detailed understanding of the various factors underlying the SCO phenomenon.

In this report, we describe the initial success of such an approach. Briefly, exposure of single crystals of Fe(tpa)$(NCS)_2$ to methanol vapor caused a dramatic yellow-to-red color change (Figure 1), suggesting that spin transitions occur in the Fe(II) centers. Subsequent crystallographic studies established the structure of a new compound, formulated as $\{[Fe(tpa)(NCS)_2]\cdot[Fe(tpa)(NCS)_2\cdot CH_3OH]\}$ (**2**), whose asymmetric unit contains two crystallographically independent molecules of Fe(tpa)$(NCS)_2$, one of which featuring strong hydrogen-bonding interaction with a methanol molecule. Magnetic measurements revealed a one-step, incomplete spin-transition process of compound **1** with some minor difference from the literature report for the same compound. However, the studies of **2** showed a two-step process with a full cycle of spin transition from HS−HS to LS−LS by way of an unambiguous LS−HS intermediate state. Guided by the

(6) (a) Halder, G. J.; Kepert, C. J.; Moubaraki, B.; Murray, K. S.; Cashion, J. D. *Science* **2002**, *298*, 1762–1765. (b) Halder, G. J.; Kepert, C. J. *Aust. J. Chem.* **2006**, *59*, 597–604. (c) Amoore, J. J. M.; Kepert, C. J.; Cashion, J. D.; Moubaraki, B.; Neville, S. M.; Murray, K. S. *Chem.—Eur. J.* **2006**, *12*, 8220–8227. (d) Neville, S. M.; Leita, B. A.; Halder, G. J.; Kepert, C. J.; Moubaraki, B.; Létard, J. F.; Murray, K. S. *Chem.—Eur. J.* **2008**, *14*, 10123–10133.

(7) (a) Nihei, M.; Han, L. Q.; Oshio, H. *J. Am. Chem. Soc.* **2007**, *129*, 5312–5313. (b) Ni, Z. P.; Shores, M. P. *J. Am. Chem. Soc.* **2009**, *131*, 32–33. (c) Leita, B. A.; Neville, S. M.; Halder, G. J.; Moubaraki, B.; Kepert, C. J.; Létard, J. F.; Murray, K. S. *Inorg. Chem.* **2007**, *46*, 8784–8795.

(8) (a) Klingele, M. H.; Moubaraki, B.; Cashion, J. D.; Murray, K. S.; Brooker, S. *Chem. Commun.* **2005**, 987–989. (b) Herbstein, F. H. *Acta Crystallogr.* **2006**, *B62*, 341–383. (c) Klingele, M. H.; Moubaraki, B.; Cashion, J. D.; Murray, K. S.; Brooker, S. *Chem. Commun.* **2005**, 987–989. (d) Muñoz, M. C.; Gaspar, A. B.; Galet, A.; Real, J. A. *Inorg. Chem.* **2007**, *46*, 8182–8192.

(9) (a) Chernyshov, D.; Hostettler, M.; Tornroos, K. W.; Burgi, H. B. *Angew. Chem., Int. Ed.* **2003**, *42*, 3825–3830. (b) Leita, B. A.; Neville, S. M.; Halder, G. J.; Moubaraki, B.; Kepert, C. J.; Letard, J. F.; Murray, K. S. *Inorg. Chem.* **2007**, *46*, 8784–8795. (c) Matouzenko, G. S.; Luneau, D.; Molnar, G.; Ould-Moussa, N.; Zein, S.; Borshch, S. A.; Bousseksou, A.; Averseng, F. *Eur. J. Inorg. Chem.* **2006**, 2671–2682.

(10) (a) Hinek, R.; Spiering, H.; Schollmeyer, D.; Gutlich, P.; Hauser, A. *Chem.—Eur. J.* **1996**, *2*, 1427–1434. (b) Hibbs, W.; van Koningsbruggen, P. J.; Arif, A. M.; Shum, W. W.; Miller, J. S. *Inorg. Chem.* **2003**, *42*, 5645–5647. (c) Bhattacharjee, A.; van Koningsbruggen, P. J.; Hibbs, W.; Miller, J. S.; Gütlich, P. *J. Phys.: Condens. Matter* **2007**, *19*, 406202/1–406202/10. (d) Bonnet, S.; Siegler, M. A.; Sánchez Costa, J.; Molnar, G.; Bousseksou, A.; Spek, A. L.; Gamez, P.; Reedijk, J. *Chem. Commun.* **2008**, 5619–5621.

(11) (a) Murray, K. S. *Eur. J. Inorg. Chem.* **2008**, 3101–3121. (b) Real, J. A.; Bolvin, H.; Bousseksou, A.; Dworkin, A.; Kahn, O.; Varret, F.; Zarembowitch, J. *J. Am. Chem. Soc.* **1992**, *114*, 4650–4658.

(12) (a) Højland, F.; Toftlund, H.; Yde-Andersen, S. *Acta Chem. Scand.* **1983**, *A37*, 251–257. (b) Paulsen, H.; Grünsteudel, H.; Meyer-Klaucke, W.; Gerdan, M.; Grünsteudel, H. F.; Chumakov, A. I.; Rüer, R.; Winkler, H.; Toftlund, H.; Trautwein, A. X. *Eur. Phys. J.* **2001**, *B23*, 463–472.

(13) (a) Bartel, M.; Absmeier, A.; Jameson, G. N. L.; Werner, F.; Kato, K.; Takata, M.; Boca, R.; Hasegawa, M.; Mereiter, K.; Caneschi, A.; Linert, W. *Inorg. Chem.* **2007**, *46*, 4220–4229. (b) Hostettler, M.; Tornroos, K. W.; Chernyshov, D.; Vangdal, B.; Burgi, H. B. *Angew. Chem., Int. Ed.* **2004**, *43*, 4589–4594.

Table 1. Crystal Data and Structure Refinements for **1** and **2**

	1 at 120 K	**1** at 260 K	**2** at 120 K	**2** at 298 K	**2** at 350K
spin state	LS	HS	LS−LS	HS−LS	HS−HS
formula	$C_{20}H_{18}N_6S_2Fe_1$			$C_{41}H_{40}N_{12}OS_4Fe_2$	
M_r/g mol^{-1}	462.37			956.78	
cryst syst	monoclinic			triclinic	
space group	$P2_1/c$			$P\bar{1}$	
a/Å	11.946(1)	12.179(1)	9.396(1)	9.597(2)	9.645(2)
b/Å	11.727(2)	11.878(1)	15.443(2)	15.714(3)	15.711(4)
c/Å	17.331(2)	17.713(1)	15.718(2)	15.890(3)	16.161(4)
α/deg			74.12(2)	73.60(2)	74.30(4)
β/deg	91.76(2)	93.39(2)	87.74(1)	86.86(2)	87.94(3)
γ/deg			75.86(2)	76.10(2)	76.83(4)
V/Å^3	2426.65(12)	2557.85(11)	2126.0(2)	2231.2(3)	2285.0(2)
Z	4	4	2	2	2
D_c/g cm^{-1}	1.271	1.201	1.490	1.420	1.386
F(000)	952	952	982	982	982
final R indices [$I > 2\sigma(I)$]	0.0869	0.0588	0.0393	0.0504	0.0429
R indices (all data)	0.2467	0.0739	0.0641	0.0708	0.0629

results from the magnetic studies, crystallographic studies have been carried out, and two crystallographically independent SCO complex units have been revealed. The spin states of the Fe(II) centers have been correlated with the structural parameters, namely, bond lengths and angles involving the metal centers, obtained at different temperatures. Most importantly, the intermediate state has been crystallographically resolved with one of the SCO sites in LS and the other in HS configuration. The oxidation and spin states of the iron centers have further been verified by variable-temperature ^{57}Fe Mössbauer spectroscopy. Details of these studies are summarized in this report.

Experimental Section

General Considerations. All reagents were purchased from Aldrich and used as received. X-ray powder diffraction (XRD) studies were performed using a Panalytical X-Pert PRO diffractometer with Cu Kα radiation ($\lambda = 0.15418$ nm, 40.0 kV, 30.0 mA). Magnetic measurements were carried out with a Quantum Design SQUID MPMS magnetometer working in the 2−360 K range with a magnetic field of 5000 Oe. Using an EasyLab Mcell 10 hydrostatic pressure cell for the Quantum Design MPMS measurement platform, pressure was applied externally to the samples. ^{57}Fe Mössbauer spectroscopic studies were performed on a Wissel MVT-1000 Mössbauer spectrometer with ^{57}Co/Rh source in the transmission mode. All isomer shifts are given relative to α-Fe at room temperature. The measurements at low temperature were performed with a closed-cycle helium refrigerator cryostat (Iwatani Co., Ltd.).

Synthesis of Compound 1. Powder sample **1** was prepared by adopting a literature procedure.[12] Layering ethanol onto a 1 mL DMF solution containing 30 mg of **1** produced yellow, X-ray quality single crystals in about two weeks. Anal. Calcd for $C_{20}H_{18}N_6S_2Fe$ (%): C 51.95; N 18.18; H 3.92. Found: C 51.67; N 17.85; H 3.77. IR (KBr, cm^{-1}): 3434.8, 2076.6, 2058.3, 1602.5, 1479.0, 1438.6, 757.1.

Preparation of Compound 2. Compound **2** was obtained, in either powder or single crystal form, by immersing compound **1** in a CH_3OH/C_2H_5OH (v/v = 1:1) mixture for 30 min under N_2 or by exposure of compound **1** to methanol vapor. Anal. Calcd for $C_{41}H_{40}N_{12}OS_4Fe_2$ (%): C 51.47; H 4.21; N 17.57. Found: C 51.65; H 4.04; N 17.42. IR (KBr, cm^{-1}): 3440.9, 2098.7, 2077.2, 2063.5, 1601.8, 1570.9, 1480.9, 1439.9, 765.9.

Crystallographic Data Collection and Structure Determination. Diffraction data for **1** (0.6 × 0.45 × 0.3 mm) were collected on an Oxford Gemini S Ultra diffractometer using Mo Kα ($\lambda = 0.71073$ Å) radiation. A single crystal of **1** was first cooled in a flow of liquid nitrogen to 120 K, and diffraction data were collected. The sample was then warmed to 260 K, and a second data set was collected. Diffraction data of **2** (0.2 × 0.15 × 0.1 mm) were collected in a similar fashion, first at 120 K and then at 298 and 350 K. Empirical absorption corrections were applied to all data using CrysAlis RED. The structures were solved using SHELXS-97 and refined using SHELXL-97.[14] All non-hydrogen atoms were refined anisotropically, and hydrogen atoms were generated using the riding model. Crystallographic data and structural refinement details are presented in Table 1. Selected bond distances and angles, as well as parameters showing salient features of the structures, are summarized in Table 2.

Results and Discussion

In this work, we sought the modification of SCO properties of a well-researched mononuclear complex, $Fe(tpa)(NCS)_2$, by heterogeneously introducing methanol molecules into the preexisting crystalline lattice of **1** where extensive hydrogen-bonding interactions between individual complex units exist. Participation of an absorbed methanol molecule in competitive hydrogen bonding with the complex units results in not only the alteration of the crystal structure but also intriguing magnetic and SCO properties of the newly formed compound, $\{[Fe(tpa)(NCS)_2]\cdot[Fe(tpa)(NCS)_2\cdot CH_3OH]\}$ (**2**), that are distinctly different from their nonsolvated parent **1**.

Magnetic Studies. The magnetic susceptibilities of **1** and **2** measured in an applied field of 5000 Oe over the temperature range 300−2 and 360−2 K, respectively, are shown in the form of plots of $\chi_M T$ versus T.

For **1**, the $\chi_M T$ value remains essentially constant at 3.53 cm^3 K mol^{-1} between 250 and 300 K, indicating an HS state (Figure 2, top). Upon cooling, the $\chi_M T$ value decreases and reaches a value of 1.90 cm^3 K mol^{-1} at 150 K. Between this temperature and 10 K there is a wide plateau, following which a sudden decrease of $\chi_M T$ value occurs. This behavior is most likely due to the zero-field effect of the residual HS-Fe(II) centers. Interestingly, a small hysteresis loop of ca. 3 K appears at about 160 K, significantly higher than the corresponding value (106 K) obtained using a powder sample.[12] The sensitivity of a compound's SCO properties to sample preparation has previously been reported.[15] For example, similar to the present observation, different SCO transition behaviors have been

(14) (a) Altomare, A.; Burla, M. C.; Camalli, M.; Cascarano, G. L.; Giacovazzo, C.; Guagliardi, A.; Moliterni, A. G. G.; Polidori, G.; Spagna, R. *J. Appl. Crystallogr.* **1999**, *32*, b115−119. (b) Sheldrick, G. M. *SHELXL-97, Program for refinement of crystal structures*; University of Göttingen: Göttingen, Germany, 1997.

Table 2. Selected Bond Lengths (Å) and Structural Parameters of **1** and **2** at Various Temperatures

bonds and angles	**1** (120 K)	**1** (260 K)	**2** (120 K)	**2** (298 K)	**2** (350 K)
Fe(1)−N(1)	2.071(5)	2.191(3)	1.962(3)	2.169(4)	2.170(2)
Fe(1)−N(2)	2.036(5)	2.201(3)	1.958(2)	2.188(3)	2.204(2)
Fe(1)−N(3)	2.067(4)	2.204(3)	1.961(3)	2.149(3)	2.186(2)
Fe(1)−N(4)	2.098(4)	2.237(3)	1.990(2)	2.234(3)	2.252(2)
Fe(1)−N(5)	1.974(6)	2.058(3)	1.946(2)	2.055(3)	2.055(2)
Fe(1)−N(6)	2.017(5)	2.116(4)	1.959(2)	2.089(4)	2.099(3)
Fe(2)−N(7)			1.952(2)	2.005(3)	2.127(2)
Fe(2)−N(8)			1.948(2)	2.016(3)	2.150(2)
Fe(2)−N(9)			1.944(2)	2.016(3)	2.116(2)
Fe(2)−N(10)			1.988(2)	2.068(3)	2.205(2)
Fe(2)−N(11)			1.948(3)	1.959(4)	2.033(3)
Fe(2)−N(12)			1.959(2)	2.015(4)	2.093(3)
$\langle d_{Fe1-N}\rangle$[a]	2.044(5)	2.168(3)	1.963(2), LS	2.164(3), HS	2.161(2), HS
$\langle d_{Fe2-N}\rangle$			1.957(2), LS	2.013(3), LS	2.121(2), HS
Σ_{Fe1}[deg]/Σ_{Fe2}[deg]	69.9	96.3	40.9/42.8	88.7/56.8	91.3/82.3
$\pi-\pi$ interactions	4.177(2)	3.987(3)	4.340(4)/	4.275(6)/	4.286(2)/
within Fe1/Fe2 layers [Å]			4.004(2)	4.224(2)	4.475(3)
S···H−C interaction	2.810(2)	2.944(3)	2.822(2)	2.977(3)	3.071(2)
within Fe1 layer [Å]	3.050(3)	3.039(2)			
	3.112(3)	3.016(2)			
S···H−C interaction			2.994(2), 3.023(2)	2.980(2), 3.021(2)	3.050(2), 2.956(2)
within Fe2 layer [Å]					
S···H−C interaction			2.797(2), 2.715(3)	2.777(2), 2.926(2)	2.827(2), 2.907(2)
between Fe1 and Fe2 [Å]			2.901(2), 3.000(2)	2.951(2), 3.077(2)	3.035(2), 3.049(2)
S···H−O interaction [Å]			2.537(2)	2.605(2)	2.719(2)

[a] $\langle d_{Fe-N}\rangle$ is the average Fe−N distance.

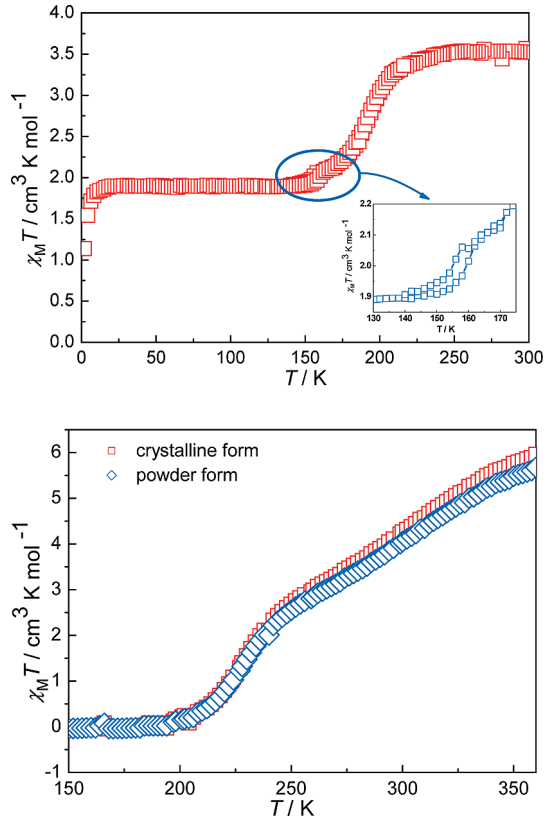

Figure 2. $\chi_M T$ vs T plots of **1** (top) and **2** (bottom).

reported for the as-synthesized and recrystallized samples of [Fe(bapbpy)(NCS)$_2$].[15] Though intriguing, the reason the complexes show such different behaviors remains unclear, but has been interpreted in terms of the slightly different chemical compositions or impurities, or defects in the crystal lattice.[15] The $\chi_M T$ values between 300 and 50 K suggest that the HS ↔ LS transition is incomplete, which is consistent with the conclusion drawn on the basis of crystallographic data at 120 K (see below).

Compound **2** displays a two-step spin-transition process separated by a narrow plateau with the transition temperature at 303 and 229 K (Figure 2, bottom), respectively. The existence of three phases with different spin states is thus suggested. At 360 K, the $\chi_M T$ value is 6.21 cm^3 K mol^{-1}, corresponding to an HS(Fe1)−HS(Fe2) state. The plateau between the two-step transitions is so narrow that it can be regarded as an inflection point. The $\chi_M T$ value at 260 K, the intermediate inflection point, is 3.16 emu K mol^{-1}, suggesting an authentic HS−LS state. The $\chi_M T$ value continues to decrease upon further temperature lowering, and a complete transition from the intermediate HS−LS state to an LS(Fe1)−LS(Fe2) state is reached at approximately 180 K. The different SCO properties shown by different forms of compound **1** prompted us to perform the magnetic measurements of **2** using both its crystalline and powder samples. However, the SCO behaviors shown are essentially the same for these two different forms (Figure 2, bottom).

Spin-transition properties of SCO compounds can be effectively modified with the application of hydrostatic pressure. Applying an external pressure favors the formation of the LS state and an increase in transition temperature.[16] As shown in Figure 3, when pressure is applied to a sample of **1**, the one-step incomplete spin transition is transformed to a two-step process, and the inflection point is about 166 K, suggesting that the residual HS-Fe(II) species under ambient pressure is able to show spin-transition behavior when additional pressure is

(15) (a) Gütlich, P. *Angew. Chem., Int. Ed.* **1994**, *33*, 2024–2054. (b) Bonnet, S.; Molnár, G.; Sánchez Costa, J.; Siegler, M. A.; Spek, A. L.; Bousseksou, A.; Fu, W. T.; Gamez, P.; Reedijk, J. *Chem. Mater.* **2009**, *21*, 1123–1136. (c) König, E.; Madeja, K. *Inorg. Chem.* **1967**, *6*, 48–55.

(16) (a) Gütlich, P.; Gaspar, A. B.; Garcia, Y.; Ksenofontov, V. *C. R. Chim.* **2007**, *10*, 21–36. (b) Gütlich, P.; Ksenofontov, V.; Gaspar, A. B. *Coord. Chem. Rev.* **2005**, *249*, 1811–1829.

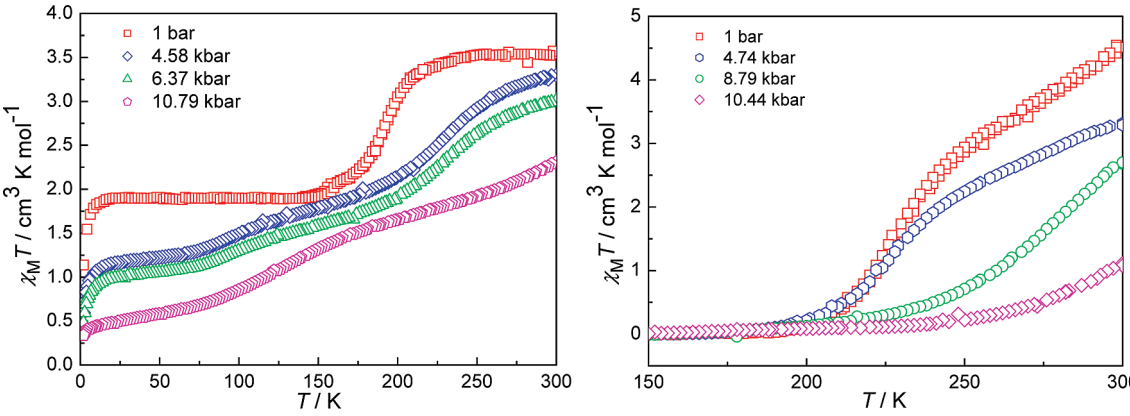

Figure 3. Pressure effects on the SCO behaviors of **1** (left) and **2** (right), respectively.

applied. With the further increase of the external pressure, an increase in transition temperature (184 and 216 K) is also observed.

For **2**, the spin transition between HS(Fe1)−HS(Fe2) and LS(Fe1)−LS(Fe2) states can also be completed under additional pressure, accompanied by an increase in the transition temperature. Interestingly, the inflection point disappears upon pressure increase, and the two-step spin transition becomes a single-step process, just the opposite of the spin-transition behavior of **1** under pressure. The pressure effects observed for **1** and **2** suggest that additional pressure strengthens the ligand field around the Fe(II) ions and minimizes the difference of chemical environments between adjacent Fe(II) sites. The pressure effect is particularly revealing in the case of compound **2**, whose solid-state structure features two distinctly different Fe sites (chemical environments). External pressure caused the two different Fe sites to behave more like each other and toward a more LS-like structure. As such, its two-step SCO transition under ambient pressure becomes a one-step process upon applying pressure, as observed.

Crystallographic Studies. Overall, the structure of the mononuclear complex unit is as expected: The Fe(II) center is hexacoordinate with coordination N atoms from two cis-disposed NCS^- groups and tris(2-pyridylmethyl)amine (tpa), the tetradentate tripodal ligand.[17] It is the intercomplex interactions and the interactions between the complex unit and absorbed methanol molecule in **2** that set apart these two solid-state structures and, more importantly, determine their SCO behaviors and associated magnetic properties.

Crystal Structure of 1. Complex **1** crystallizes in the monoclinic space group $P2_1/c$. Its asymmetric unit contains one complete Fe(tpa)$(NCS)_2$ molecule (Figure 4). For the structure determined at 120 K, the Fe−N bond lengths range from 1.977(8) to 2.091(6) Å with an average of 2.044(5) Å. This value is slightly longer than that typical of an LS-Fe(II)−N bond, suggesting an incomplete SCO transition at this particular temperature. The corresponding value measured at 260 K is 2.168(3) Å, falling in the range typical of an HS-Fe(II)−N bond. These spin-state assignments made on the basis of Fe−N bond distances are consistent with those based on the octahedral distortion parameter (Σ),[18] a parameter commonly used for the quantification of the angular deviation of an octahedron from an ideal octahedral geometry. A smaller Σ value is generally associated with a stronger ligand field and, therefore, an LS state of the metal ion, while the opposite suggests an HS state.[18,19] In the present case, the Σ values are 69.94° and 96.33° at 120 and 260 K, respectively, suggesting that the ligand field at the lower temperature is stronger than the one at the higher temperature.

The crystal packing of **1** can be described as a 2-D supramolecular array of the complex units (Figure 4). Along the [010] direction are chains stabilized by both $\pi-\pi$ interactions between pyridine rings on adjacent complex units and S···H−C hydrogen bonding.[6c,d] The aromatic centroid-to-centroid distances are 4.177(2) Å (120 K) and 3.987 Å (260 K). The slightly closer $\pi-\pi$ separation at 260 K causes a small decrease of the Fe···Fe separation to 6.942(1) Å from 6.984(2) Å at 120 K. For the S···H−C hydrogen bonding, the S···H separation is 2.810 and 2.944 Å at 120 and 260 K, respectively. Individual 1-D chains are associated along the [100] direction by the S···H−C hydrogen bonding to form the observed 2-D crystal packing; the S···H separation ranges from 3.050(3) to 3.112(3) Å at 120 K and from 3.016(2) to 3.039(2) Å at 260 K. These two sets of S···H distances are longer than the corresponding values of the S···H−C hydrogen bonding along the [010] direction.

Crystal Structure of 2. Crystal data of **2** were collected at 120, 298, and 350 K in order to correlate the structures at different temperatures with the three different SCO phases, the HS−HS, LS−HS, and LS−LS, identified by the magnetic studies described above. The compound, formulated as {[Fe(tpa)$(NCS)_2$]·[Fe(tpa)$(NCS)_2$·CH_3OH]}, crystallizes out in the space group $P\bar{1}$. Its asymmetric unit features two crystallographically distinct molecules, Fe(tpa)$(NCS)_2$ (Fe1 site) and Fe(tpa)$(NCS)_2$·CH_3OH (Fe2 site) (Figure 5).

Clearly, the transformation from **1** to **2** is induced by the incorporation of the absorbed methanol molecule that is strongly associated with one NCS^- group at the Fe2 site via S···H−O hydrogen bonding. Not only are such interactions responsible for the distinct crystal packing of **2** with respect to that of **1** (Figure 1, right), they are also responsible for the observed molecular distortion, in particular about the Fe2 site.[20] Specifically, although the four NCS^- groups in the two complex units are almost linear, the Fe2−N−C linkages are appreciably bent,

(17) Matouzenko, G. S.; Bousseksou, A.; Lecocq, S.; Koningsbruggen, P. J. van.; Perrin, M.; Kahn, O.; Collet, A. *Inorg. Chem.* **1997**, *36*, 2975–2981.

(18) Guionneau, P.; Marchivie, M.; Bravic, G.; Létard, J. F.; Chasseau, D. *J. Mater. Chem.* **2002**, *12*, 2546–2551.

(19) Guionneau, P.; Marchivie, M.; Bravic, G.; Létard, J. F.; Chasseau, D. *Top. Curr. Chem.* **2004**, *234*, 97–128.

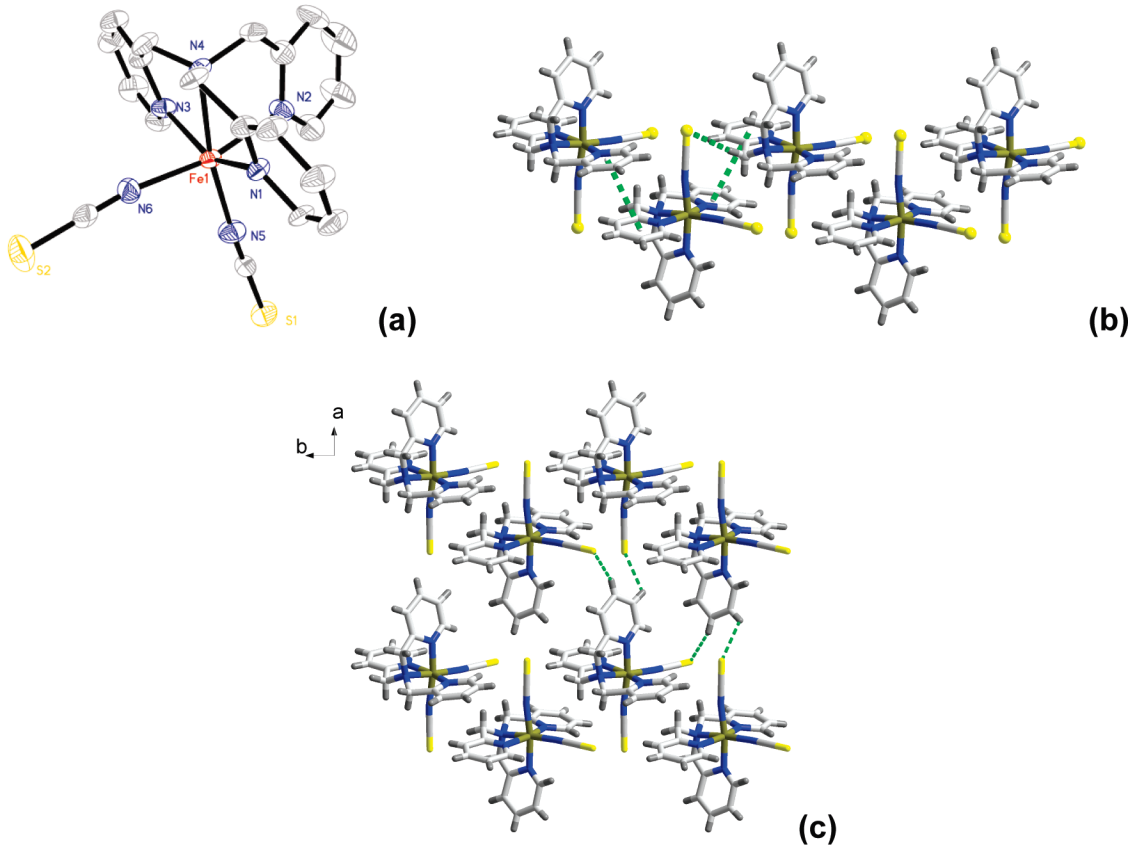

Figure 4. ORTEP drawing (30% probability) of the crystal structure of **1** (a); $\pi-\pi$ and S···H−C interactions in the 1-D chain viewed along the *b* axis in **1** (b); and 2-D layer structure of **1** showing the hydrogen-bond interactions between the 1-D chains (c).

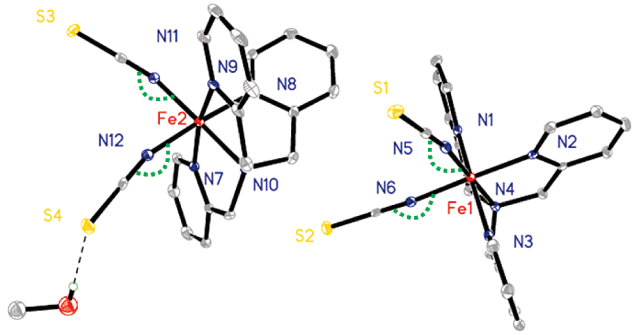

Figure 5. ORTEP drawing (30% probability) of the two complex units present in the asymmetric unit of the crystal structure of compound **2**.

and the C−N12−Fe2 and C−N11−Fe2 angles are much smaller than the C−N5−Fe1 and C−N6−Fe1 angles (Table 3).

At 120 K, the average Fe−N bond lengths (1.963(2) and 1.957(2) Å) and Σ values (40.9° and 42.8°) for Fe1 and Fe2, respectively, suggest that both Fe centers are of an LS configuration, and the crystal is in the LS(Fe1)−LS(Fe2) phase. The corresponding values at 298 K increase sizably to 2.164(3) Å and 88.7° at the Fe1 site, whereas those associated with the Fe2 site increase only marginally to 2.013(3) Å and 56.8°. The change of 0.201 Å in the Fe1−N bond length falls in the range typical of an LS-to-HS transition, suggesting that an LS-to-HS transition occurs at the Fe1 site upon temperature change.[19,21] In other words, compound **2** exists as an intermediate

Table 3. Selected Bond Angles (deg) of the Two Isomeric Units in **2**

	120 K	298 K	350 K
N(5)−C(19)−S(1)	179.4(3)	178.8(4)	179.0(3)
N(6)−C(20)−S(2)	179.5(3)	179.5(4)	179.7(3)
N(11)−C(39)−S(3)	178.7(3)	177.6(5)	178.9(4)
N(12)−C(40)−S(4)	179.1(3)	178.7(5)	178.6(3)
C(19)−N(5)−Fe(1)	171.1 (2)	163.6(4)	165.1(3)
C(20)−N(6)−Fe(1)	174.7(2)	174.3(4)	174.4(2)
C(39)−N(11)−Fe(2)	165.0(3)	163.7(4)	156.0(3)
C(40)−N(12)−Fe(2)	165.1(2)	163.3(4)	159.7(3)
N1−Fe1−N3	166.95(9)	152.58(14)	152.17(9)
N4−Fe1−N5	179.26(10)	172.20(12)	171.76(9)
N2−Fe1−N6	176.38(9)	169.69(12)	169.20(9)
N7−Fe2−N9	167.35(11)	161.97(17)	154.47(10)
N8−Fe2−N12	174.42(10)	172.62(16)	169.31(10)
N10−Fe2−N11	179.00(10)	178.85(16)	174.95(11)

HS(Fe1)−LS(Fe2) phase at 298 K. At 350 K, the corresponding metric values at the Fe1 site, 2.161 Å and 91.3°, change only slightly with respect to their counterparts measured at 298 K, whereas the parameters at the Fe2 site increase significantly to 2.121 Å and 82.3°, respectively, corresponding to an HS configuration; compound **2** now exists in the HS(Fe1)−HS(Fe2) phase. Here, the X-ray structural analysis reveals the nature of the complete two-step transition in **2** as being successive from [LS−LS] (120 K) to [HS−HS] (350 K) via a unique [LS−HS] intermediate phase with two distinct SCO centers of different spin configurations. We note that examples of direct crystallographic resolution of an intermediate HS−LS phase in a

(20) (a) Real, J. A.; Muñoz, M. C.; Andàes, E.; Granier, T.; Gallois, B. *Inorg. Chem.* **1994**, *33*, 3587–3594. (b) Bréfuel, N.; Duhayon, C.; Shova, S.; Tuchagues, J. P. *Chem. Commun.* **2007**, 5223–5225.

(21) Gallois, B.; Real, J.-A.; Hauw, C.; Zarembowitch, J. *Inorg. Chem.* **1990**, *29*, 1152–1158.

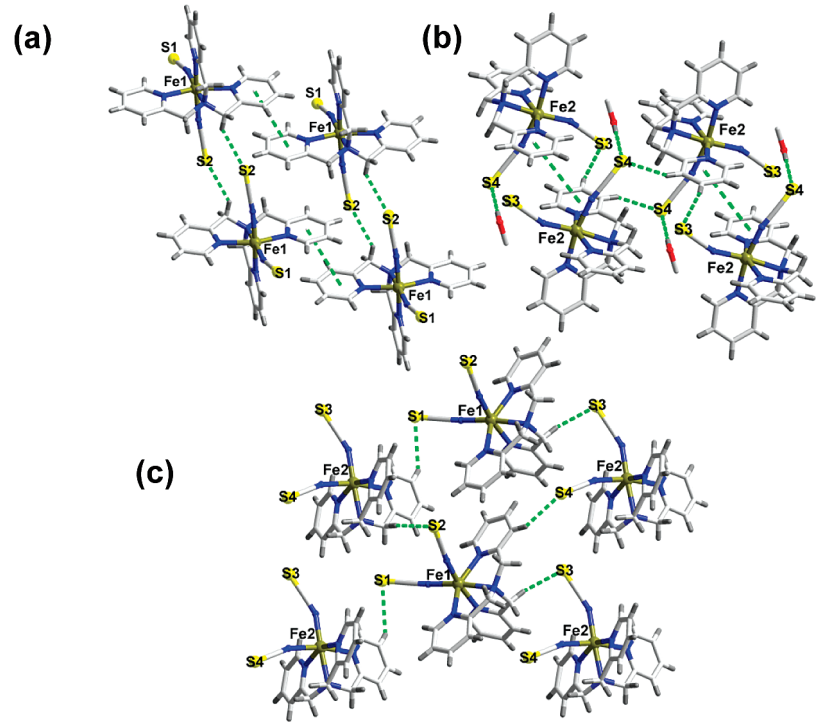

Figure 6. Supramolecular interactions in the structure of **2**: (a) within the Fe1 molecular layer, (b) within the Fe2 molecular layer, and (c) between the Fe1 and Fe2 layers.

monomeric complex, especially that exist all over the transition temperature regions, are rare and that the present approach to achieve such a state through deliberately manipulating the supramolecular interactions between SCO centers, as opposed to the usual means of changing temperature or pressure, or the brute-force methods of changing counteranions of the complexes or crystallization solvents, is unprecedented.[9,10]

Compound **2** displays a compact 3-D supramolecular structure in the solid state with alternate Fe1 and Fe2 molecular layers interlinked by multiple S···H−C hydrogen-bonding interactions. Within the Fe1 layer (Figure 6a), there exist $\pi-\pi$ and S···H−C (methylene group of the tpa ligand) interactions, just as in the case of **1**. The centroid-to-centroid distance of the $\pi-\pi$ interaction is 4.340(4) Å at 120 K and decreases upon temperature increase, while the S···H separation in the hydrogen-bonding interaction measures at 2.822(2) Å and increases upon temperature increase. Within the Fe2 layer (Figure 6b), the $\pi-\pi$ interaction with a centroid-to-centroid distance of 4.004(2) Å at 120 K strengthens with increasing temperature, just the opposite of what is observed in the Fe1 layer. However, the S···H−C (benzene ring) interactions do not show any obvious temperature dependence. Probably most salient is the change of S···H distance of the S···H−O hydrogen-bonding interaction involving the absorbed methanol molecules and the SCN^- groups: The closest distances of S···H−O are 2.537(2), 2.605(2), and 2.719(2) Å at 120, 298, and 350 K, respectively. The sensitive temperature dependence of this parameter underscores the importance of the absorbed methanol in affecting the spin transition behavior of the Fe2 center.[6] A direct consequence of the hydrogen bonding involving methanol is a stronger communication between the Fe2 sites: The shortest Fe2···Fe2 separations of 8.154(1), 8.203(2), and 8.177(2) Å are much shorter than the corresponding Fe1···Fe1 distances of 8.620(1), 8.893(1), and 9.040 Å at 120, 298, and 350 K, respectively. The different chemical environments around the Fe1 and Fe2 centers are probably responsible for the distinct spin-transition behaviors associated with these two sites.[15,22] There are also multiple S···H−C (methylene group) and S···H−C (benzene ring) interactions between the Fe1 and Fe2 layers (Figure 6c). The closest Fe1···Fe2 separation is measured at 7.984(1), 8.188(2), and 8.404(2) Å at 120, 298, and 350 K, respectively. No obvious cooperativity is observed in the process of spin transition, and conversion of HS and LS states at each Fe(II) center takes place independently.

It should be noted, however, that although the change in intermolecular cooperativity of compound **1** versus that of **2** is rationalized exclusively in the present work in terms of the altered intermolecular interactions (hydrogen-bonding and aromatic−aromatic interactions), it has recently been shown that electrostatic contributions (change of Madelung field along the spin transitions) significantly enhance the cooperativity factor and probably should have been taken into account.[5a,b] Quantitative analysis of this important factor by *ab initio* calculations should constitute a meaningful research topic in our future research.[5]

Mössbauer Spectroscopy. ^{57}Fe Mössbauer spectroscopy can be used to determine the oxidation and spin states of iron atoms in complexes and is sensitive to structural changes in the coordination sphere.[15,23] In the present work, the studies were carried out using microcrystalline samples of **2** from 300 to 16 K, shown in Figure 7. The hyperfine parameters were obtained by least-squares fitting to the Lorentzian lines, and correlative parameters at different temperature are collected in Table 4.

(22) Gütlich, P.; Jung, J.; Goodwin, H. A. Spin transition in iron(II) complexes. In *Molecular Magnetism: from molecular assemblies to the devices*; Coronado, et al., Eds.; NATO Advance Study Institute Series E321; Plenum: New York, 1996; p 327.
(23) Grunert, C. M.; Reiman, S.; Spiering, H.; Kitchen, J. A.; Brooker, S.; Gütlich, P. *Angew. Chem., Int. Ed.* **2008**, *47*, 2997–2999.

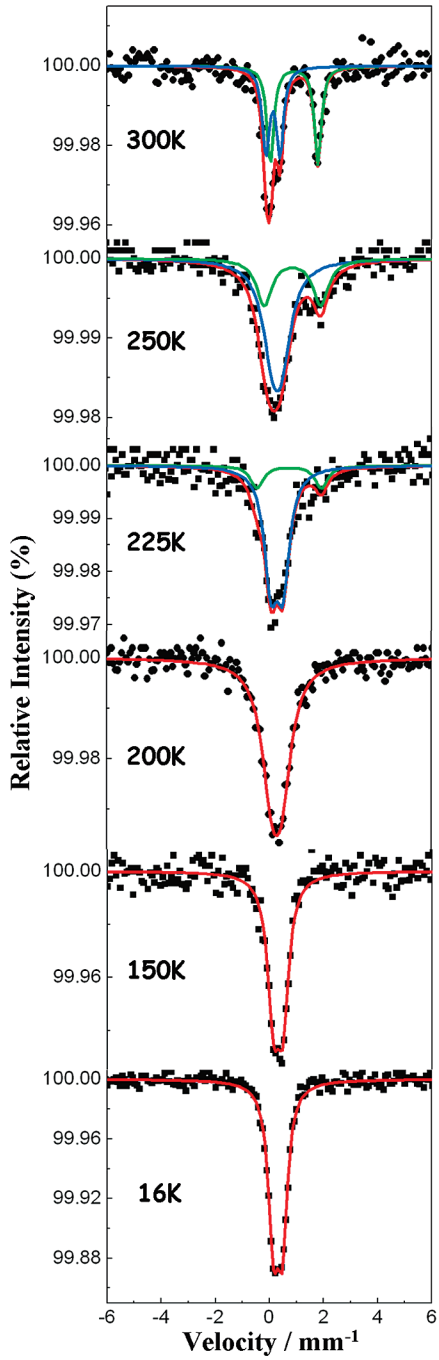

Figure 7. Temperature-dependent ^{57}Fe Mössbauer spectra of polycrystalline **2**.

According to the crystallographic results described above, the Fe1 and Fe2 centers are both situated in an octahedral geometry. At 300 K, the Fe1 center is in an HS configuration, while the Fe2 center possesses both HS and LS characters. Therefore, the main doublet (red line) can be ascribed to a combination of HS and LS Fe(II) ions, with the HS ion showing a relatively high quadrupole splitting ($\Delta E_Q = 1.76$ mm s^{-1}) and isomer shift ($\delta = 0.91$ mm s^{-1}) and the LS ion having smaller values of these parameters ($\Delta E_Q = 0.52$ mm s^{-1} and $\delta = 0.13$ mm s^{-1}). The area fractions of the HS and LS components are 53.1% (green line) and 46.9% (blue line), respectively. This conclusion is consistent with the results obtained from the crystallographic analysis and the magnetic studies. As the temperature is decreased, the resonance lines start to broaden, and the intensity of the LS doublet increases at the expense of the HS doublet, suggesting thermally induced HS(Fe1)-to-LS(Fe2) transition; at 250 K the HS and LS quadrupole splittings are $\delta = 0.85$ mm s^{-1} and $\Delta E_Q = 2.08$ mm s^{-1} (area fraction 32.4%) for HS and $\delta = 0.28$ mm s^{-1} and $\Delta E_Q = 0.35$ mm s^{-1} (area fraction 67.6%) for LS, respectively. On further lowering the temperature to 225 K, where the Fe1 and Fe2 sites are both in the LS states as suggested by the structural data, the spectra are dominated by an LS Fe(II) quadrupole doublet with $\delta = 0.28$ mm s^{-1} and $\Delta E_Q = 0.38$ mm s^{-1} (82.6%), while possessing a low percentage of HS Fe(II) $\delta = 0.73$ mm s^{-1} and $\Delta E_Q = 2.38$ mm s^{-1} (17.4%). As the temperature is lowered to 200 K and further to 16 K, the LS fraction reaches the value of 100% (area fraction), consistent with the results of the magnetic studies and suggesting a complete spin transition from LS to HS configuration. Clearly, these results from Mössbauer spectroscopic studies are in line with the nature of the two-step spin-transition process, as established by the above crystallographic and magnetic studies.

Table 4. Mössbauer Spectroscopic Parameters Characterizing Spin State of Fe(II) in Compound **2**

	isomer shift (mm s^{-1})		quadrupole splitting (mm s^{-1})		area fraction (%)	
	HS	LS	HS	LS	HS	LS
300 K	0.91	0.13	1.76	0.52	53.1	46.9
250 K	0.85	0.28	2.08	0.35	32.4	67.6
225 K	0.73	0.28	2.38	0.45	17.4	82.6
200 K		0.28		0.38		100
150 K		0.31		0.35		100
16 K		0.31		0.33		100

Summary

We report herein the single-crystal-to-single-crystal transformation of a well-studied SCO complex by means of solvent molecule sorption. The competitive hydrogen bonding of the absorbed methanol with the SCO complex units disrupts the original supramolecular interactions, resulting in two crystallographically distinct SCO centers with which an intermediate HS−LS state along the complete [HS−HS] ↔ [LS−LS] transition pathway has been identified. Comparative studies have been carried out using magnetic measurements, X-ray crystallography, and Mössbauer spectroscopy, with which the spin-transition behaviors and associated magnetic properties of the original complex **1** and the solvent-incorporating complex **2** have been investigated in detail. It has been found that in this mononuclear SCO complex system, the original, incomplete one-step HS ↔ LS spin transition process has now been transformed into a complete, two-step process comprised of HS−HS, HS−LS, and LS−LS phases. Compound **2** represents a rare example of mononuclear SCO complexes for which a clearly defined intermediate HS−LS state can be resolved crystallographically. This study offers much desired insight into the nature of the interactions between individual SCO centers in the solid state and, most importantly, illustrates the power of manipulating supramolecular interactions in modifying materials properties. It is tempting to submit that the spin-transition behavior and associated properties such as color and magnetism of various SCO complexes, including those that are otherwise well-studied, may be modified systematically by supramolecular means for the possible production

of advanced molecule-based materials with unique SCO behaviors and magnetic properties.[24]

Acknowledgment. We thank Prof. Yasuaki Einaga of Keio University for the measurement of Mössbauer spectra. This work was supported by the NNSF of China (Grant 20721001, 20971106, 90922012), NCET-08-0470 of MOE, the NSF of Fujian Province (Distinguished Young Scientists, Grant 2009J06006), and the 973 Project (Grant 2007CB815301).

Supporting Information Available: Crystal photo and XRD spectra and the crystal data (CIF) are available free of charge via the Internet at http://pubs.acs.org.

JA909695F

(24) (a) Brooker, S.; Kitchen, J. A. *Dalton Trans.* **2009**, 7331–7340. (b) Gamez, P.; Sánchez Costa, J.; Quesadaa, M.; Aromí, G. *Dalton Trans.* **2009**, 7845–7853.